CRISPR-mediated reversion of oncogenic KRAS mutation results in increased proliferation and reveals independent roles of Ras and mTORC2 in the migration of A549 lung cancer cells

Alyssa N. Werner[b], Avani I. Kumar[b], and Pascale G. Charest[a,b,c,*]
[a]Department of Molecular and Cellular Biology, and [b]Department of Chemistry and Biochemistry, University of Arizona, Tucson, AZ 85721; [c]University of Arizona Cancer Center, Tucson, AZ 85721

ABSTRACT Although the *RAS* oncogene has been extensively studied, new aspects concerning its role and regulation in normal biology and cancer continue to be discovered. Recently, others and we have shown that the mechanistic Target of Rapamycin Complex 2 (mTORC2) is a Ras effector in *Dictyostelium* and mammalian cells. mTORC2 plays evolutionarily conserved roles in cell survival and migration and has been linked to tumorigenesis. Because *RAS* is often mutated in lung cancer, we investigated whether a Ras–mTORC2 pathway contributes to enhancing the migration of lung cancer cells expressing oncogenic Ras. We used A549 cells and CRISPR/Cas9 to revert the cells' *KRAS* G12S mutation to wild-type and establish A549 revertant (REV) cell lines, which we then used to evaluate the Ras-mediated regulation of mTORC2 and cell migration. Interestingly, our results suggest that K-Ras and mTORC2 promote A549 cell migration but as part of different pathways and independently of Ras's mutational status. Moreover, further characterization of the A549^{REV} cells revealed that loss of mutant K-Ras expression for the wild-type protein leads to an increase in cell growth and proliferation, suggesting that the A549 cells have low *KRAS*-mutant dependency and that recovering expression of wild-type K-Ras protein increases these cells tumorigenic potential.

Monitoring Editor
Matthew Welch
University of California, Berkeley

Received: May 2, 2023
Revised: Sep 8, 2023
Accepted: Sep 11, 2023

Cross-Validation

SIGNIFICANCE STATEMENT

- mTORC2 is an evolutionarily conserved Ras effector influencing cell survival, migration, and tumorigenesis. A role for Ras–mTORC2 in lung cancer cells with KRAS mutations is not known. Using CRISPR/Cas9 gene editing, the authors reverted the KRAS mutations of A549 lung cancer cells and studied its impact on the cells' growth and mTORC2-mediated migration.
- They found that the A549 revertant cells grow faster and that A549 cells migrate using distinct K-Ras and mTORC2 pathways, independently of KRAS's mutational status.
- These findings highlight the presence of context-dependent Ras and mTORC2 pathways and possible undesirable outcomes of genetically correcting KRAS mutations in cancer.

This article was published online ahead of print in MBoC in Press (http://www.molbiolcell.org/cgi/doi/10.1091/mbc.E23-05-0152) on September 20, 2023.

Conflict of Interest: The authors declare that the research was conducted in the absence of any commercial or financial relationships that could be construed as a potential conflict of interest.

Author Contributions: A.N.W. and P.G.C. conceived experiments and wrote the manuscript; A.N.W. and A.I.K. conducted the experiments. All authors analyzed the results and reviewed the manuscript.

*Address correspondence to: Pascale G. Charest (pcharest@arizona.edu).

Abbreviations used: CA, constitutively active; CRISPR, clustered regularly interspaced short palindromic repeats; CXCL12, CXC-motif chemokine ligand 12; CXCR4, CXC chemokine receptor 4; EGF, epidermal growth factor; EGFR, EGF receptor; ERK, extracellular signal-regulated kinase; FACS, fluorescence assisted cell sorting; MAP, mitogen-activated protein; mTOR, mechanistic target of rapamycin; mTORC1, mTOR complex 1; mTORC2, mTOR complex 2; NT, non-targeting; NSCLC, non-small cell lung cancer; PI3K, phosphoinositide 3-kinase; REV, revertant; sgRNA, single guide RNA; siRNA, small interfering RNA; ssODN, single-stranded oligodeoxynucleotide.

INTRODUCTION

Ras proteins are evolutionarily conserved and act as molecular switches in cells, cycling between GTP-bound active and GDP-bound inactive states (Bourne *et al.*, 1991; Pylayeva-Gupta *et al.*, 2011; Simanshu *et al.*, 2017). The human Ras isoforms K-, H-, and N-Ras have been extensively studied due to their involvement in tumorigenesis, with ~20% of tumors expressing an activating mutation in one of these Ras proteins (Omerovic *et al.*, 2008; Rhett *et al.*, 2020). Most commonly, mutations cluster around the nucleotide-binding site at codons 12, 13, and 61, leading to enhanced GTP binding and, consequently, a Ras constitutively active (CA) phenotype (Muñoz-Maldonado *et al.*, 2019; Prior *et al.*, 2020). Notably, lung cancers have one of the highest rates of Ras mutation, with ~30% of non–small cell lung cancers (NSCLCs) expressing a K-Ras CA mutant (Cerami *et al.*, 2012; Gao *et al.*, 2013; Westcott and To, 2013; Westcott *et al.*, 2015; Zhu *et al.*, 2017; Lindsay *et al.*, 2018; Prior *et al.*, 2020). Canonical Ras effectors include phosphoinositide 3-kinase (PI3K) leading to activation of AKT, and Raf1 leading to activation of the extracellular-regulated kinases (ERK) 1 and 2, thereby promoting cell survival and proliferation, respectively (Gimple and Wang, 2019; Lavoie *et al.*, 2020; Rathinaswamy and Burke, 2020). In addition, increasing evidence indicates that Ras also plays important roles in promoting the migration and invasion of cells by acting through several pathways, including PI3K and ERK, as well as the p38 mitogen-activated protein (MAP) kinase, and mechanistic Target of Rapamycin Complex 2 (mTORC2; Moon *et al.*, 2000; Kim *et al.*, 2003; Lee *et al.*, 2016; Yoh *et al.*, 2016; Gimple and Wang, 2019; Smith *et al.*, 2020; Soriano *et al.*, 2021; Collins *et al.*, 2023).

mTORC2 plays an evolutionarily conserved role in cell migration and has been shown to contribute to metastasis in many cancer types (Kim *et al.*, 2017; Xie *et al.*, 2018). mTORC2 is one of two well-characterized signaling complexes containing the Ser/Thr kinase mTOR (Zhou and Huang, 2010). mTORC1 and mTORC2 have distinct substrates and functions, which are determined by their specific components, including Rictor for mTORC2 and Raptor for mTORC1. mTORC1 has been extensively studied and is an established master regulator of cell growth and proliferation (Liu and Sabatini, 2020). However, the signaling mechanisms and pathways that lead to mTORC2 activation and cell migration are incompletely understood. In the experimental model *Dictyostelium discoideum*, others and we have shown that the small GTPase Ras activates mTORC2 to promote cell migration (Sasaki and Firtel, 2006; Kamimura *et al.*, 2008, p. 3; Cai *et al.*, 2010; Charest *et al.*, 2010; Liao *et al.*, 2013; Khanna *et al.*, 2016; Pal *et al.*, 2023). Work with neutrophils and different human cancer cells has since shown that the Ras-mediated regulation of mTORC2 is conserved in humans, and that mTORC2 is a direct effector of oncogenic mutant Ras proteins (Kovalski *et al.*, 2019; Lone *et al.*, 2019; Pal *et al.*, 2023). Moreover, we recently demonstrated that both wild-type (WT) and oncogenic Ras promote mTORC2 activation and the mTORC2-dependent migration and invasion of transformed breast epithelial cells (Collins *et al.*, 2023). Here, we sought to define the role of Ras and mTORC2 in lung cancer cells harboring an oncogenic *RAS* mutation.

RESULTS

Lung cancer cell models to interrogate the effect of oncogenic Ras on mTORC2 function

To investigate the role of the Ras–mTORC2 pathway in lung cancer cells expressing an oncogenic K-Ras mutant, we chose the commonly used human NSCLC cell line A549, which is homozygous for the *KRAS* mutation c.34G>A (G12S; Blanco *et al.*, 2009; Tate *et al.*, 2019). To help address the specific effect of K-Ras CA expression on regulating mTORC2 function in these cells, we used a CRISPR/Cas9 gene knock-in approach with a single-strand oligodeoxynucleotide (ssODN) as the donor template to revert the K-Ras G12S mutation and create A549 cells that express only WT *KRAS* alleles (Figure 1A; Chen *et al.*, 2011; Bialk *et al.*, 2015). For this, we used two different *KRAS* gene targeting single guide RNAs (sgRNAs) predicted to have limited and different potential off-targets (Supplemental Figure S1), as well as a nontargeting (NT) sgRNA as control. We transiently transfected the CRISPR/Cas9 vectors, which also encode the ZsGreen fluorescent protein that allowed us to sort the transfected A549 cells by fluorescence-assisted cell sorting (FACS; Supplemental Figure S2). We then isolated clones by limiting dilution and verified the *KRAS* sequences by Sanger sequencing. We selected one clone for each sgRNA used and termed them A549 NT ($A549^{NT}$; control cell line homozygous for *KRAS* G12S), and A549-revertant (REV) clones 1 and 2 ($A549^{REV1}$, $A549^{REV2}$; A549 cell lines homozygous for WT *KRAS*; Figure 1B).

K-Ras REV A549 cells display increased cell growth and proliferation

Before investigating the effect on cell migration, we evaluated the consequence of reverting the *KRAS* oncogenic mutation on the proliferation of A549 cells. For this, we first assessed the growth of the $A549^{REV}$ cell lines compared with that of A549 and $A549^{NT}$ cells in colony formation assays. Interestingly, we observed that both $A549^{REV1}$ and $A549^{REV2}$ formed ~1.6× more colonies than the control cells when grown as 2D monolayers (Figure 2A). Using a 3D soft-agar tumorigenicity assay, which allows evaluating the anchorage-independent cell proliferation potential, we also observed that both $A549^{REV}$ cell lines generated significantly larger colonies than those formed by $A549^{NT}$ cells ($A549^{REV1}$ and $A549^{REV2}$ colonies, ~110 μm; $A549^{NT}$ colonies, ~85 μm; Figure 2B). To then further characterize the cell growth and proliferation phenotype of the $A549^{REV}$ cells, we assessed cell growth using a quantitative MTT assay (Carmichael *et al.*, 1987). In this assay, the $A549^{REV}$ cells displayed ~2× more cell growth, further supporting that these cells have an increased proliferative potential (Figure 2C). Interestingly, treatment with rapamycin, a well-characterized inhibitor of mTORC1 and cell growth, led to significant inhibition of the revertant cells' growth while it did not affect the control cells, suggesting that the increased proliferative potential of the revertant cells is dependent on the mTORC1 pathway (Figure 2D). Importantly, the comparison of the $A549^{NT}$ cells to the unmodified A549 cells revealed comparable cell growth, which suggests that the CRISPR procedure did not select for cells with an increased proliferation phenotype and, thus, that this is not likely to be an artifact of the procedure.

We then investigated whether knocking down K-Ras CA expression has a similar effect to reverting the mutation. For this, we performed the siRNA-mediated silencing of K-Ras in A549 cells and compared their cell growth, as measured in a quantitative MTT assay, to that of cells treated with K-, H-, and N-Ras siRNAs (Pan-Ras siRNAs) or a NT control siRNA (Supplemental Figure S3). Interestingly, we observed a tendency of increased cell growth for cells with the K-Ras knockdown and of decreased cell growth for cells with all three main Ras knocked down (Figure 2E). Whereas the difference between the two knockdown conditions is statistically significant, neither of them were found to be statistically different from the NT siRNA–treated control cells. Nonetheless, this result suggests that silencing K-Ras CA in A549 cells produces a negligeable effect on the growth of the cells, which is a different outcome than that of correcting the mutations to WT K-Ras in the revertant cells.

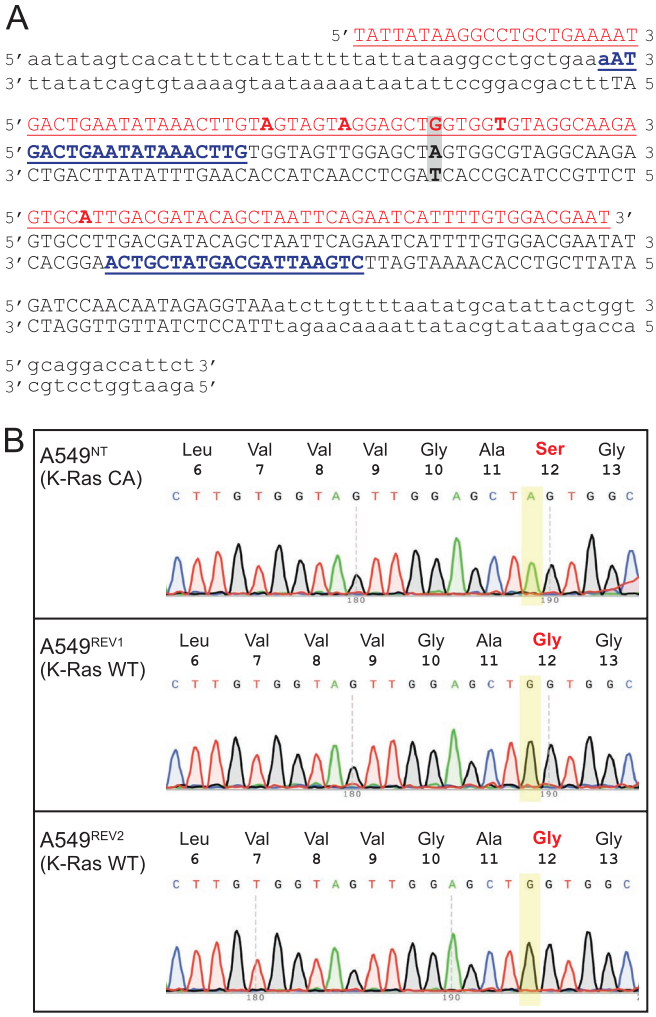

FIGURE 1: Reverting the K-Ras CA mutation of A549 cells. (A) CRISPR/Cas9 strategy to change nucleotide 34 A>G of K-Ras (indicated by shading) and, thereby, revert the G12S mutation back to Glycine at amino acid position 12. In black: K-Ras genomic sequence with the coding sequence in capital letters. In red: ssODN sequence, with PAM sequence mutations (to prevent further sgRNA targeting) indicated by bold letters. In blue: sgRNA-1 (forward) and sgRNA-2 (reverse) sequences. (B) Sequencing results confirming the reverting of the K-Ras G12S CA mutation to WT in A549 cells by sgRNA-1 ($A549^{REV1}$) and sgRNA-2 ($A549^{REV2}$). The sequencing also confirmed that the K-Ras G12S CA mutation is intact in cells treated with the sgRNA-NT control.

K-Ras promotes A549 cell migration

To investigate the effect of the K-Ras CA mutations on A549 cell migration, we assessed the migration of the revertant cells compared with that of $A549^{NT}$ using a 2D wound closure assay. Interestingly, we found the measured wound closures to be very similar between the $A549^{NT}$, $A549^{REV1}$, and $A549^{REV2}$ cells (Figure 3A), suggesting comparable migratory potentials. We then further investigated the role of K-Ras CA and the other two main Ras isoforms H- and N-Ras in A549 cell migration using siRNA-mediated silencing (Supplemental Figure S3). We observed that silencing K-Ras alone in $A549^{NT}$, $A549^{REV1}$, and $A549^{REV2}$ cells similarly reduced the migration of the cells by ~30%, suggesting a role for K-Ras independently of its mutational status (Figure 3B). We also observed that silencing H- and N-Ras in addition to K-Ras reduced the measured cell migration even more, by ~50%. However, because the silencing of all three Ras proteins has a stronger effect on cell growth (Figure 2E), it is possible that this contributes to the observed measured wound closure. Therefore, these findings suggest that K-Ras plays a role in the migration of A549 cells independently of its mutational status, whereas a role for the other WT Ras proteins is less clear.

mTORC2 promotes A549 cell migration

To investigate the role of mTORC2 in A549 cell migration, because there are no currently available mTORC2-selective inhibitors, we first compared the effect of inhibiting both mTORC1 and mTORC2 using the mTOR inhibitor PP242 to that of inhibiting only mTORC1 using the mTORC1-selective inhibitor rapamycin (Supplemental Figure S4A; Janes *et al.*, 2010; Tee, 2018). In a 2D wound-healing migration assay, we observed that rapamycin treatment has no effect on the migration of $A549^{NT}$ cells, whereas it reduced the migration of the revertant cells, although it was found only to be statistically significant for $A549^{REV2}$ (Figure 4A). Because we found that rapamycin significantly inhibits the revertant cells' growth (Figure 2D), its effect on the wound-healing assay likely reflects the contribution of cell proliferation to the measured would closure. We do not know the reason for these different rapamycin sensitivities on the revertant cells' migration, but these could be due to some clonal variation between them (see *Discussion*). Nonetheless, this observation suggests a minimal overall role of mTORC1 and/or cell growth in the measured migration of the A549 strains. On the other hand, inhibition of both mTORC1 and mTORC2 by PP242 led to comparably strong decreases in cell migration for the $A549^{NT}$ and the revertant cells (>80%), suggesting a role for mTORC2 in the migration of all three strains.

To more specifically inhibit mTORC2 function, we also assessed the effect of siRNA-mediated silencing of the mTORC2 unique and essential component Rictor on the migration of A549 cells (Supplemental Figure S4B). Although we were able to achieve less than 70% Rictor knockdown (cells retained more than 30% Rictor expression), we observed that this was sufficient to cause significant and comparable decreases in the migration of revertant and control cells (Figure 4B). Consequently, the fact that only partial inhibition of mTORC2 function by Rictor siRNA knockdown leads to a significant reduction of cell migration further indicates that mTORC2 promotes A549 cell migration.

To then evaluate the role of mTORC2 in the 3D migration of A549 cells, we assessed the effect of inhibiting mTORC2 function on the migration of cells in a transwell invasion assay. First, we observed comparable migration of the revertant cells and control cells, further suggesting that reverting the *KRAS* mutations in A549 cells does not affect the cells' migration ability (Figure 4C). We also observed that rapamycin treatment (mTORC1 inhibition) shows a tendency to reduce the migration of all three strains, although only the effect on $A549^{NT}$ cells shows statistical significance. Because proliferation is expected to have minimal effect on this type of 3D migration assay, this observation suggests a potential role for mTORC1 in regulating the invasive behavior of A549 cells. Importantly, we observed that inhibition of both mTORC1 and mTORC2 by PP242 greatly reduced the migration of all three strains to comparable extents, and considerably more so than mTORC1 inhibition alone. When considering all three migration experiments together, the results indicate that mTORC2 mediates A549 cell migration and that this role is independent of K-Ras's mutational status.

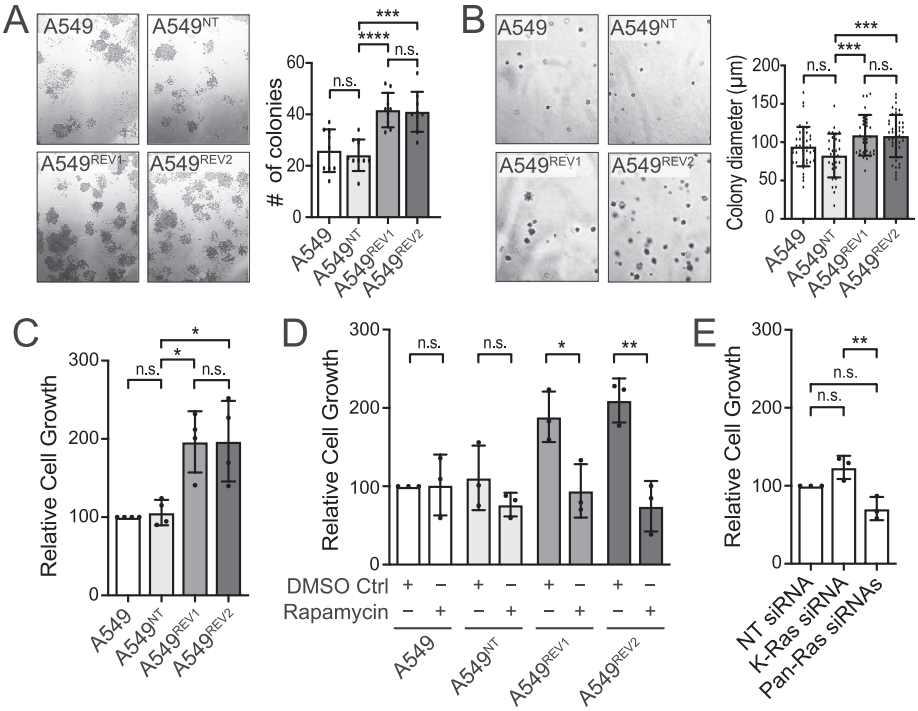

FIGURE 2: Cell growth and proliferation are increased in the K-Ras revertant A549 cells. (A) 2D colony-formation assay performed with the A549^{NT}, A549^{REV1}, and A549^{REV2} cells as described in *Materials and Methods*. Representative images of three independent experiments are shown. Data on the graph represent the average number of colonies of nine replicates from three independent experiments ± SD ($n = 9$). (B) 3D soft agar tumorgenicity assay performed as described in *Materials and Methods*. Representative images of three independent experiments are shown. Data on the graph represent the measured diameter of every colony in a field of view from three independent experiments ± SD ($n = 27–37$ colonies). (C) MTT assay comparing cell growth in the different strains, performed as described in *Materials and Methods*. Data on the graph represent measurements from four independent experiments normalized to the control A549 cells ± SD ($n = 4$). (D) MTT assay performed with cells pretreated with 10 µM rapamycin or 0.1% DMSO as control (Ctrl). Data on the graph represent measurements from three independent experiments normalized to the A549^{NT} DMSO control ± SD ($n = 3$). (E) MTT assay performed on cells treated with NT, K-Ras, or Pan-Ras siRNAs. Data on the graph represent measurements from three independent experiments normalized to the control NT siRNA condition ± SD ($n = 3$). Adjusted p values: * $p < 0.05$; ** $p < 0.01$; *** $p < 0.001$; **** $p < 0.0001$. ns, nonstatistically significant.

mTORC2 activity in A549 cells is regulated independently of Ras

To investigate the regulation of mTORC2 by K-Ras CA in A549 cells, we used the mTORC2-dependent phosphorylation of AKT at S473 as a read-out for mTORC2 activity in log-phase growing cells, which we compared with that of ERK phosphorylation as a read-out for the activity of the canonical Ras–MAPK pathway. First, we confirmed that A549^{NT}, A549^{REV1}, and A549^{REV2} have similar levels of AKT, ERK, and total Ras protein expression, suggesting that the CRISPR/Cas9 procedure and/or the loss of Ras-CA expression did not affect these genes' expression levels (Supplemental Figure S5A). We observed that phosphorylation levels of both AKT(S473) and ERK in A549^{REV1} and A549^{REV2} are comparable to those in A549^{NT} control cells (Figure 5A; Supplemental Figure S5B). Because we confirmed that pAKT(S473) is dependent on mTORC2 in these cells (Supplemental Figure S4), this observation indicates that K-Ras CA expression does not affect mTORC2 nor ERK activity in growing A549 cells.

To then examine the potential Ras-mediated regulation of mTORC2 in response to a stimulus in A549 cells, we assessed the effect of chemotactic cytokine CXC-motif chemokine ligand 12 (CXCL12) and epidermal growth factor (EGF) stimulations on the activity of mTORC2 in serum-starved cells. Both CXCL12, EGF, and their respective receptors CXC chemokine receptor 4 (CXCR4) and EGF receptor (EGFR), have been linked to lung cancer and evidence suggest that they can promote lung cancer cell migration (Phillips *et al.*, 2003; Mitsudomi and Yatabe, 2010; Lauand *et al.*, 2013; Xie *et al.*, 2014; Appert-Collin *et al.*, 2015; Pawig *et al.*, 2015; Wang *et al.*, 2016; Liu *et al.*, 2017; Zuo *et al.*, 2017). On one hand, we observed that CXCL12 stimulation induces little or no phosphorylation of AKT, nor of ERK, in any of the A549 cell lines, suggesting that there is either little CXCR4 receptor or that it just does not significantly activate the AKT and ERK pathways in these cells (Supplemental Figure S5C). On the other hand, EGF induced a strong and comparable pAKT(S473) response in A549^{NT}, A549^{REV1}, and A549^{REV2} (Figure 5B), and a weaker but reproducible pERK response (Supplemental Figure S5D). We then assessed the effect of EGF on A549 cell migration and observed that EGF stimulation significantly induces cell migration, which was inhibited by treatment with the mTORC1/mTORC2 inhibitor PP242 and not by the mTORC1-selective inhibitor rapamycin, suggesting that EGF promotes A549 cell migration through mTORC2 (Figure 5C). Moreover, we found that EGF stimulated the migration of A549^{NT}, A549^{REV1}, and A549^{REV2} in a comparable manner, indicating that K-Ras CA does not contribute to promoting the migration of cells in response to EGF (Figure 5D).

Because we found evidence suggesting an important role for K-Ras in A549 cell migration independently of its mutation (Figure 3B), we tested its role in promoting mTORC2 activation in response to EGF stimulation using siRNA-mediated silencing. Because K-Ras migrates a bit slower than H- and N-Ras when resolved on SDS–PAGE (Lim and Boyer, 2021; Lim and Khoo, 2021), we were able to confirm its efficient knockdown to ~85% in all three cell lines (Supplemental Figure S6A). Moreover, this quantification allowed us to confirm that A549^{NT}, A549^{REV1}, and A549^{REV2} cells have similar levels of K-Ras expression, whether it is mutated or not. We observed that silencing K-Ras alone or in combination with H- and N-Ras in all three cell lines did not inhibit the EGF-stimulated pAKT, but actually showed a tendency to increase the response although this was only found to be statistically significant for A549^{REV2} (Figure 6). On the other hand, the pan-siRNA treatment significantly reduced the EGF-induced pERK response (Supplemental Figure S6B). Consequently, these observations indicate that mTORC2 is strongly activated downstream from EGFR in A549 cells but independently of Ras.

DISCUSSION

Taken together, our study using CRISPR-mediated editing of A549 lung cancer cells to revert their oncogenic *KRAS* mutations to WT

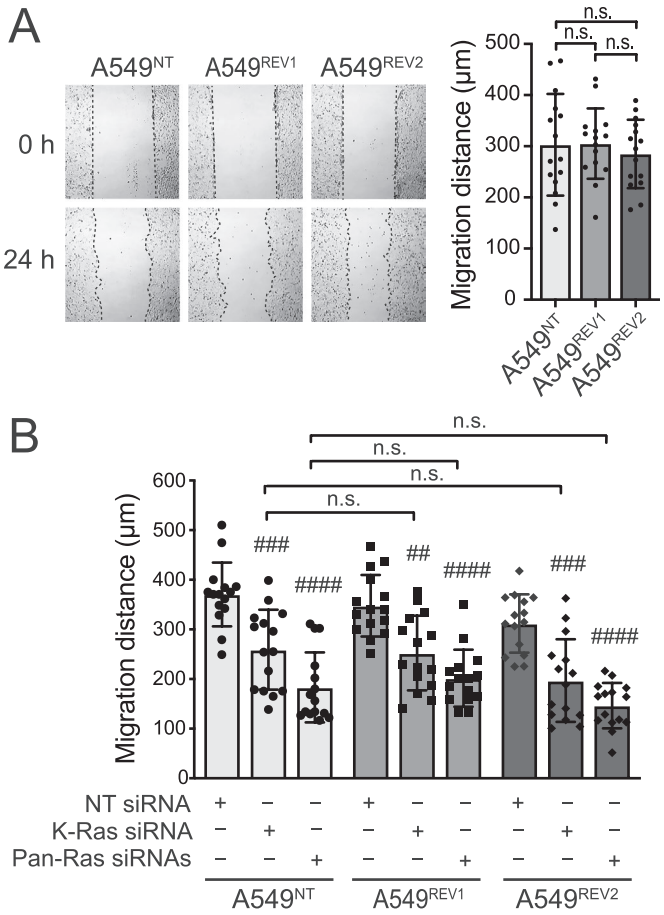

FIGURE 3: K-Ras promotes A549 cell migration independently of its mutation. (A) Wound closure cell-migration assays were performed with A549^{NT}, A549^{REV1}, and A549^{REV2} cells as described in *Materials and Methods*. Representative images of three independent experiments are shown, taken immediately after wounding (0 h) and after 24 h. Data on the graph represent measured wound closure (migration distances) in five areas of each wound from three independent experiments ± SD ($n = 15$). (B) Wound-healing migration assays were performed with A549^{NT}, A549^{REV1}, and A549^{REV2} subjected to siRNA-mediated knockdown of K-Ras alone, of K-, H-, and N-Ras (Pan-Ras siRNA) or treated with NT siRNA control. The data were analyzed and graphed as described in (A). Adjusted p values for the differences between siRNA-mediated knockdowns and the NT siRNA control for each strain: ## $p < 0.01$; ### $p < 0.001$; #### $p < 0.0001$. ns, nonstatistically significant.

reveals not only that K-Ras and mTORC2 promote the migration of these cells as part of different pathways, but that correcting the *KRAS* mutation results in an increase in the A549 cells' growth and proliferation.

The finding that genetically correcting the *KRAS* mutations in cancer cells can lead to their increased growth and proliferation and, thereby, enhanced tumorigenic potential was unexpected because *KRAS* is a well-described oncogene that is known to drive cellular transformation and tumor initiation. However, there is evidence that oncogenic K-Ras does not always continue to play a key role in later stages of cancer progression (Singh *et al.*, 2009). In fact, many cancer cells harboring *KRAS* mutations were found to have low-mutant K-Ras dependency, including the A549 lung cancer cells, although these cells are still very tumorigenic (Singh *et al.*, 2009; Weng *et al.*, 2012; Fujita-Sato *et al.*, 2015; Zhang *et al.*, 2022). In these studies, *KRAS* was either partially inhibited or knocked-down leading to little or no effects on cell proliferation, which is consistent with our observations using K-Ras siRNA-mediated silencing, which had no significant effect on cell growth compared with the complete reversion of the *KRAS* mutations.

We think that the effect of partial targeting versus complete reversion of the *KRAS* mutations on cell growth also explains the difference between ours and previous studies that used CRISPR/Cas9-edited *KRAS* G12S in A549 cells and reported reduced cell growth and viability (Gao *et al.*, 2020; Sayed *et al.*, 2022). These studies were performed with a pool of *KRAS* CRISPR/Cas9-edited A549 cells displaying ~50–75% editing efficiency and, thus, likely includes many cells that retained one mutant *KRAS* allele. In our study, the *KRAS* A549^{REV} cells are clones that are homozygous for the WT *KRAS* gene and, therefore, do not express any mutant K-Ras protein while they gained expression of the WT protein back. Therefore, altogether, these previous studies and our observations suggest that the partial targeting versus complete reversion of *KRAS* G12S in A549 cells leads to different outcomes that are likely due to the distinct effects of the WT versus mutant K-Ras in these cells. These findings then add to a growing body of evidence that WT Ras proteins play critical roles in cancer, including in *RAS*-mutant cancers, although these roles appear to vary depending on the cellular context (Zhou *et al.*, 2016; Sheffels and Kortum, 2021). Because some cancer cells *in vivo* could be similar to A549 cells, these findings highlight the possibility that targeting the Ras mutant in cancer may not only result in the absence of therapeutic effect but could even worsen the prognosis.

Although some previously reported CRISPR and cloning-related artifacts could cause increased cell growth (Giuliano *et al.*, 2019), the method that we used is designed to minimize CRISPR off-targets (only transiently expressing Cas9 and using two different sgRNAs) and the A549^{NT} cells allowed to control for potential clonal effects. We sometimes observe small differences between the two A549^{REV} cell lines, for example, in the extent to which they respond to inhibitors or stimuli. These small differences could be due to CRISPR off-target effect variations between the two strains that were produced with two different sgRNAs, and very few of them were found to be statistically significant. Consequently, because the phenotypes of A549^{NT} cells closely resemble those of the parental A549 cells, and that A549^{REV1} and A549^{REV2} have extremely similar phenotypes, we are confident that those truly result from reverting the *KRAS* mutation. Moreover, we observed similar K-Ras and total Ras expression levels in A549^{REV1} and A549^{REV2} compared with the A549^{NT} control cells, confirming that reverting the *KRAS* mutations did not change the *RAS* genes' expression levels. Therefore, we conclude that the phenotypic changes that we observed in the A549^{REV} cells are due to these cells regaining expression of the WT K-Ras protein, which in turn led to an increase in cell growth.

Because we did not detect any significant difference in AKT and ERK expression or activities between the REV and control A549 cells, our observations suggest that the mechanism underlying the increased cell growth phenotype lies in other pathways. Our finding that rapamycin significantly inhibits the increased cell growth of the revertant cells compared with the A549 control cells suggests a potential role for mTORC1, although we did not observe an increase in the phosphorylation of its substrate S6K1 (Supplemental Figure S7). However, it is possible that another branch of the mTORC1 pathway could be implicated. In an effort to identify other potential players and mechanisms involved, we assessed the expression of epithelial-to-mesenchymal transition (EMT) markers as well as the expression and activity of additional key oncogenic pathway proteins, but these

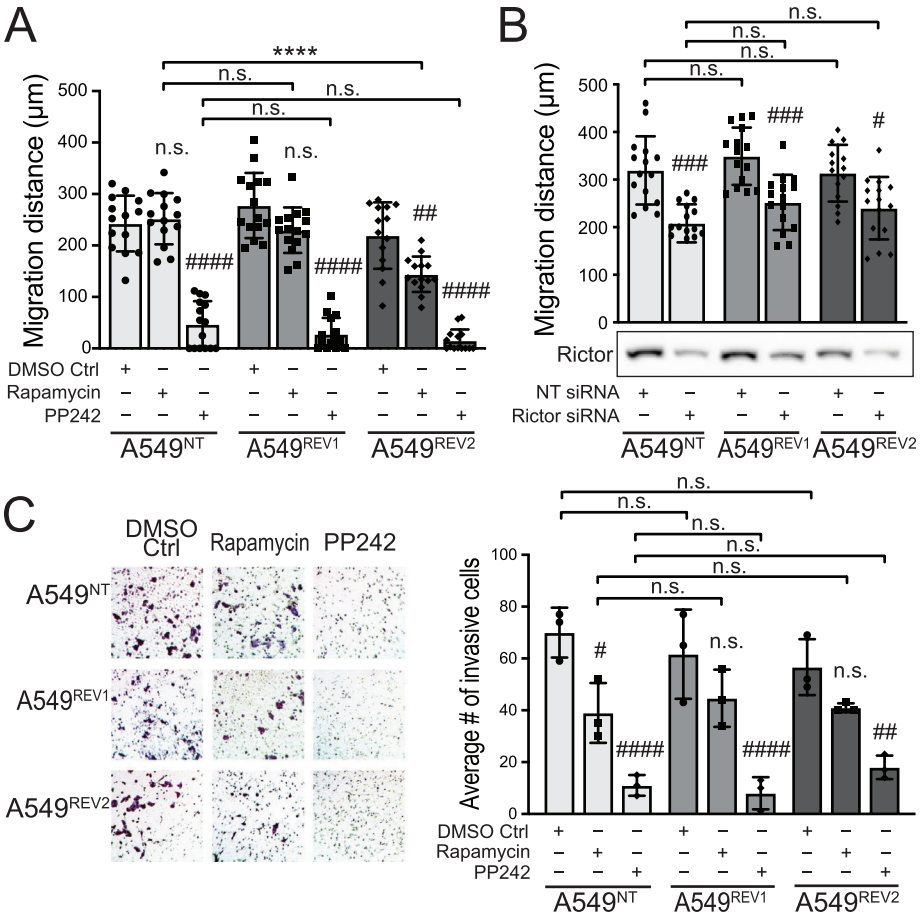

FIGURE 4: mTORC2 mediates the migration of A549 cells independently of K-Ras's mutational status. (A and B) Wound closure migration assays were performed with the A549^{NT}, A549^{REV1}, and A549^{REV2} cells treated with 10 μM rapamycin (mTORC1 inhibitor), 10 nM PP242 (mTORC1/mTORC2 inhibitor), or 0.1% DMSO control (A), or subjected to siRNA-mediated Rictor knockdown or treated with NT siRNA control (B), as described in *Materials and Methods*. Rictor immunoblots were performed to verify its siRNA-mediated knockdown and the data shown are representative of three independent experiments. Data on graphs represent measured migration distances in five areas of each wound from three independent experiments ± SD (n = 15). (C) Transwell 3D invasion assays were performed with the cells and conditions as described in (A). Representative images of three independent experiments are shown. Data on graph represent the average number of cells that have invaded per area measured from three separate experiments ± SD (n = 3). **** adjusted p value < 0.0001. Adjusted p values for the differences between treatment conditions and their respective control for each strain: #, $p < 0.05$; ##, $p < 0.01$; ###, $p < 0.001$; ####, $p < 0.0001$. ns, nonstatistically significant.

studies were also inconclusive (Supplemental Figure S7). One previous study using different cancer cells harboring distinct Ras-mutant isoforms revealed the presence of a potential negative feedback loop, driven by oncogenic Ras, that desensitizes growth factor and WT Ras signaling, and that targeting oncogenic Ras can then lead to increased signaling and tumorigenicity (Young *et al.*, 2013). It is possible that a similar feedback loop is involved in leading to the increased cell growth of the A549^{REV} cells, although we did not observe any significant increases in the signaling pathways that we assessed. Therefore, further investigations are needed to determine how reverting the *KRAS* mutations in A549 cells leads to an increase in proliferation that may involve mTORC1.

Others and we have shown that mTORC2 is an effector of oncogenic and WT Ras, although evidence suggest that the mechanism of Ras-mediated mTORC2 regulation can vary depending on the nature of the cells and stimulus (Kovalski *et al.*, 2019; Senoo *et al.*, 2019; Smith *et al.*, 2020; Collins *et al.*, 2023; Pal *et al.*, 2023; Saha *et al.*, 2023). It was thus surprising to discover that neither K-Ras CA nor WT Ras proteins regulate mTORC2 activity in A549 cells, although both K-Ras and mTORC2 are important for their migration. This finding thus further highlights context-dependent variations in cancer, where distinct types of cancer cells harboring different mutations may use significantly diverse signaling networks. One pathway through which Ras could promote A549 cell migration independently of mTORC2 is by acting through ERK, which has been previously linked to the Ras-mediated migration of lung cancer cells (Uekita *et al.*, 2014; Fan *et al.*, 2021; Liu *et al.*, 2022). As for mTORC2, its activity could be regulated by the product of PI3K, phosphatidylinositol-3,4,5-triphosphate (Gan *et al.*, 2011; Liu *et al.*, 2015; Fu and Hall, 2020; Smith *et al.*, 2020), which can be independent of Ras because PI3K can be directly activated by growth factor receptors (Fruman *et al.*, 2017). However, it is possible that other, as yet unknown, mechanisms also regulate the activity of mTORC2 and its function in A549 cells and future studies aimed at identifying those mechanisms in addition to how they possibly crosstalk with Ras signaling will be important to understand the many different ways through which mTOR and Ras can contribute to tumorigenesis.

MATERIALS AND METHODS

Request a protocol through *Bio-protocol*.

Reagents

Life Technologies Penicillin-Streptomycin, Life Technologies OptiMEM I Reduced Serum Medium, Invitrogen Lipofectamine RNAiMAX Transfection reagent, PeproTech Animal-free Recombinant Human EGF, Invitrogen MTT (3-[4,5-dimethylthiazol-2-yl]-2,5-Diphenyltetrosolium), and Corning RPMI 1640 Medium (Mod. w/o phenol red) 1X without glutamine, were purchased from Thermo Fisher Scientific (Waltham, MA). Fetal bovine serum (FBS) and PP242 were obtained from Avantor (Radnor Township, PA); RPMI-1640 media was purchased from Corning (Corning, NY); Rapamycin was obtained from Research Products International (Mt. Prospect, IL); and ProBlock Gold Protease Inhibitor Cocktail was from Gold Biotechnology (St. Louis, MI). Dharmacon ON-TARGET*plus* Non-targeting siRNA Control Pool and SMARTPool of Human H-Ras (3265), Human N-Ras (4893), and Human K-Ras (3845) were obtained from Horizon Discovery (Waterbeach, UK), and SignalSilence Control siRNA (unconjugated) and SignalSilence Rictor siRNA were purchased from Cell Signaling Technology (Danvers, MA).

Antibodies

Phospho-AKT (Ser473; 193H12) rabbit mAb, AKT (pan; 40D4) mouse mAb, and P-p44/42 MAPK (T202/Y204; pERK) rabbit mAb

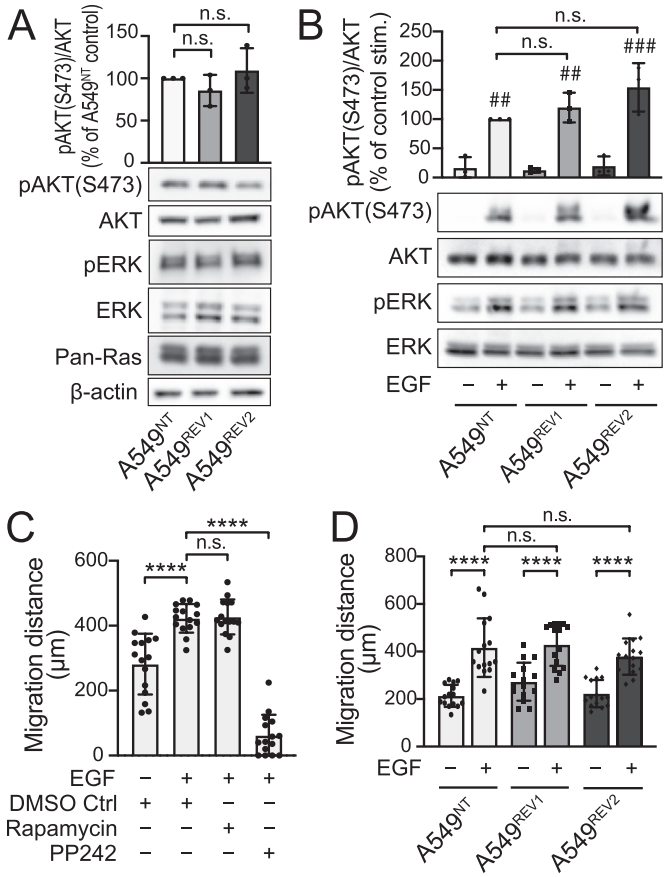

FIGURE 5: Basal and stimulus-induced mTORC2 activity in A549 cells is unaffected by the presence of mutant K-Ras. (A) Phosphorylation of mTORC2-dependent AKT S473 [pAKT(S473)] and of ERK (pERK) was assessed in log-phase growing $A549^{NT}$, $A549^{REV1}$, and $A549^{REV2}$ cells as described in *Materials and Methods*. Representative immunoblots of three independent experiments are shown. Bands were quantified by densitometry and the data on the graph represent the ratio of pAKT(S473)/AKT expressed as percentage of $A549^{NT}$ control from three separate experiments ± SD ($n = 3$). (B) pAKT(473) and pERK were assessed by immunoblot following stimulation by 100 ng/mL EGF or PBS as negative control. Representative immunoblots of three independent experiments are shown. Bands were quantified by densitometry and the data on the graph represent the ratio of pAKT(S473)/AKT expressed as percentage of $A549^{NT}$ control stimulation measured from three separate experiments ± SD ($n = 3$). Adjusted p value for the difference between control and EGF stimulation in each strain: ##, $p < 0.01$; ###, $p < 0.001$. (C) Wound closure migration assays were performed with A549 cells stimulated or not with 100 ng/mL EGF and treated with 10 µM rapamycin (mTORC1 inhibitor), 10 nM PP242 (mTORC1/mTORC2 inhibitor), or 0.1% DMSO control as described in *Materials and Methods*. Data on the graph represent measured migration distances in five areas of each wound from three independent experiments ± SD ($n = 15$). (D) Wound closure migration assays were performed with the $A549^{NT}$, $A549^{REV1}$, and $A549^{REV2}$ cells stimulated or not with 100 ng/mL EGF. Data on the graph represent measured migration distances in five areas of each wound from three independent experiments ± SD ($n = 15$). Adjusted p values: ****, $p < 0.0001$. ns, nonstatistically significant.

were purchased from Cell Signaling Technology (Danvers, MA). ERK1 (C-16) IgG rabbit mAb was purchased from Sant Cruz Biotechnology (Dallas, TX), and anti-Pan-Ras (Ab-3) Mouse Ab (Ras 10) was from MilliporeSigma (Burlington, MA). Rabbit anti-Rictor Affinity Purified mAb was purchased from Bethyl Laboratories (Montgomery, TX). Peroxidase AffiniPure Goat anti-Rabbit IgG and peroxidase AffiniPure Goat anti-Mouse IgG were purchased from Jackson ImmunoResearch Laboratories (West Grove, PA).

Cell Culture

A549 cells were obtained from the University of Arizona Cancer Center Experimental Mouse Shared Resources. The A549 and A549-derived cell lines were maintained in RPMI-1640 supplemented with 10% FBS and 100 U/mL penicillin/streptomycin (growth medium). siRNA transient transfections were performed in OptiMEM I Reduced Serum Medium using Lipofectamine RNAiMAX Transfection Reagent according to the manufacturer's protocol.

CRISPR/Cas9-mediated gene editing

The CRISPR/Cas9 constructs were designed and obtained from TransOMIC Technologies (Huntsville, AL). The CRISPR/Cas9 machinery was provided in an all-in-one vector (pCLIP-ALL-hCMV-ZsGreen) that includes a gene for expressing the fluorescent protein ZsGreen, with either NT control single guide RNA (sgRNA-NT: GGAGCGCACCATCTTCTTCA) or K-Ras targeting sgRNA-1 (CTGAATTAGCTGTATCGTCA) or K-Ras targeting sgRNA-2 (AATGACTGAATATAAACTTG). The knock-in at position 34 A>G was performed via addition of an ssODN oligo (Figure 1A). Transfection of the CRISPR/Cas9 all-in-one vector together with the ssODN was performed in OptiMEM I Reduced Serum Medium using the OMNIfect transfection reagent according to manufacturer's protocol. Cells displaying ZsGreen expression were sorted by FACS using a BD FACSAria III at the University of Arizona Flow Cytometry Shared Resource core facility. The fluorescent-sorted cells were cloned by limiting dilution in 96-well plates. The genomic DNA from three clones of each of the sgRNA-NT, sgRNA-1, and sgRNA-2 transfected cells were isolated using the Quick-DNA Miniprep Plus Kit from Zymo Research (D4068; Irvine, CA). The isolated DNA was sent for sequencing at CD Genomics (Shirley, NY).

2D Colony Formation Assay

Two-hundred cells were plated in each well of a 24-well plate and incubated for 5 d in RPMI growth medium. The colonies were fixed with 100% methanol for 20 min at 25°C and stained with 0.5% crystal violet in 25 % methanol for 5 min and washed with dH_2O. Colonies in each well were counted in five fields of view and then averaged.

3D Soft-Agar Tumorigenicity Assay

Ten-thousand cells from a cell suspension of 10,000 cell/mL in 0.3% agarose/RPMI growth medium was overlayed on 0.6% agarose/RPMI growth medium plates. The agarose was allowed to solidify for 15 min at 4°C before the plates were incubated for 1 wk at 37°C, after which the diameter of the colonies was measured.

MTT Cell Proliferation Assay

The MTT assay was performed according to Invitrogen's rapid protocol (Carmichael *et al.*, 1987). Briefly, 5000 cells were plated in each well of a 96-well cell culture plate and incubated for 24 h in RPMI growth medium before replacing the media with 100 µL of Corning RPMI 1640 Medium (mod. w/o phenol red) 1× without Glutamine. Ten microliters of a 12 mM MTT solution was added to each well (~1 mM MTT) and the cells were incubated for 4 h at 37°C. After incubation, all but 25 µL of the reaction solution was removed, and the dye was solubilized by adding 50 µL DMSO to

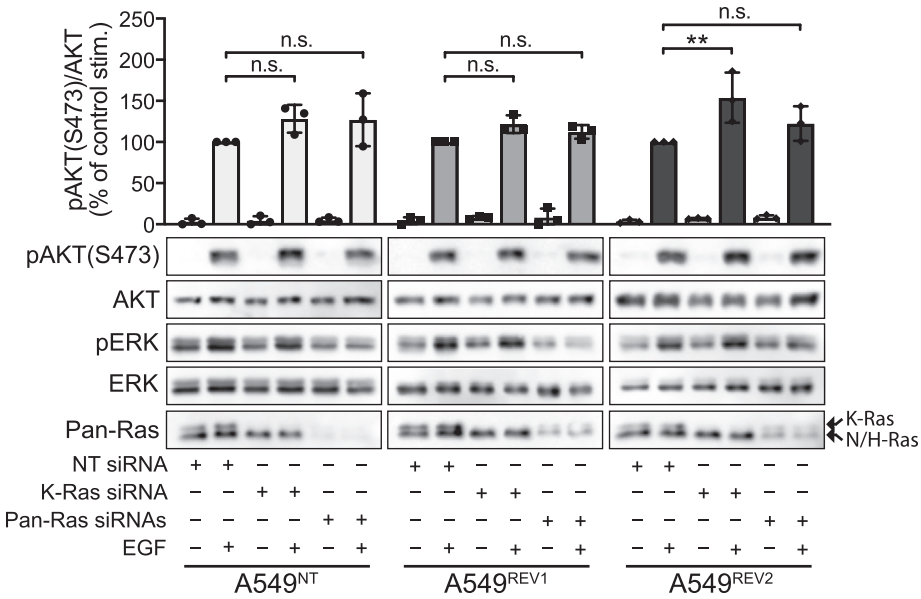

FIGURE 6: EGF stimulates mTORC2 activity independently of Ras in A549 cells. pAKT(S473) and pERK were assessed in cells pretreated with K-Ras siRNA, Pan-Ras siRNAs, or NT siRNA control, and stimulated or not with 100 ng/mL EGF as described in *Materials and Methods*. Ras knockdowns were verified by immunoblot. Representative immunoblots of three independent experiments are shown. Bands were quantified by densitometry and the data on the graph represent the ratio of pAKT(S473)/AKT expressed as percentage of $A549^{NT}$ control stimulation measured from three separate experiments ± SD ($n = 3$). Adjusted p value: **, $p < 0.01$. ns, nonstatistically significant.

each well and incubating for 10 min at 37°C followed by reading the absorbance at 540 nm.

Immunoblots

For experiments with resting cells, log-phase growing cells were collected and lysed on ice in 20 mM MOPS pH 7.0, 150 mM NaCl, 10 mM $MgCl_2$, 1 mM DTT, 0.5% NP-40, 10% Glycerol, 0.5 mM sodium orthovanadate, 50 mM NaF, 10 mM B-glycerol phosphate, supplemented with protease inhibitors. Lysates were cleared by centrifugation and samples were mixed 1:3 with 4× Laemli sample buffer containing 100 mM DTT, resolved on SDS–PAGE, and analyzed by immunoblotting. Where indicated, cells were pretreated for 2 h with 0.1% DMSO (carrier control), 10 μM rapamycin or 10 nM PP242 at 37°C. For experiments with EGF stimulation, log-phase growing cells were transferred to serum free media for 16 h, which was replaced with fresh serum-free media for 2 h before stimulation with either PBS (carrier control) or 200 ng/mL EGF for 10 min. Cells were then collected and lysed on ice as described above.

Wound Closure 2D Migration Assay

Cells were grown to confluency in 6-well plates and scratches were made manually using flat-tip pipette tips, removing a uniform, thin line of cells from one end of the well to the other. Wounds were washed to remove floating cells and contrast images were captured using a Motic Stereo Zoom microscope to measure initial wound sizes. The wounded cells were then incubated for 24 h at 37°C before capturing a second set of contrast images. Cell migration distances were determined by calculating the difference in wound sizes at the end of the incubation using the average of five wound widths for each wound, measured with the Motic Images Plus software. Where indicated, cells were treated with 0.1% DMSO, 10 μM rapamycin, or 10 nM PP242, and stimulated with PBS or 200 ng/mL EGF.

Transwell 3D Migration/Invasion Assay

Corning BioCoat Matrigel Invasion Chamber with 8.0 μm PET membrane in 24-well plates from Corning (Corning, NY) were used following the manufacturer's protocol. Briefly, 2×10^4 cells were seeded in the top chambers with growth media in both chambers and then incubated for 24 h at 37°C. Where indicated, 0.1% DMSO, 10 μM rapamycin, or 10 nM PP242 were added to both chambers. After incubation, the cells that did not migrate were removed from the upper surface of the membrane, and the cells that did migrate to the lower chamber and that were attached to the lower surface of the membrane were fixed with 3.7% formaldehyde, permeabilized with methanol, and stained with 0.5% crystal violet in 20% ethanol. Using a light microscope, the stained cells were counted across five different fields of view encompassing the center and edges of the membranes.

Statistical analyses

All quantified data were graphed and analyzed in Prism using the one-way ANOVA statistical test followed by post hoc multiple comparison analysis with the Bonferroni correction. The adjusted p values are indicated in the figure legends, and a p of 0.05 was considered the statistically significant threshold.

ACKNOWLEDGMENTS

This work was supported by a National Institutes of Health R01 grant GM131200 to P.G.C. and A.N.W. was also supported by National Institutes of Health T32 grant GM008804. Gene editing and cell sorting were performed with the assistance of the University of Arizona Experimental Mouse Shared Resources (EMSR) and Flow Cytometry Core, respectively.

REFERENCES

Appert-Collin A, Hubert P, Crémel G, Bennasroune A (2015). Role of ErbB Receptors in Cancer Cell Migration and Invasion. Front Pharmacol 6, 283.

Bialk P, Rivera-Torres N, Strouse B, Kmiec EB (2015). Regulation of Gene Editing Activity Directed by Single-Stranded Oligonucleotides and CRISPR/Cas9 Systems. PLOS ONE 10, e0129308.

Blanco R, Iwakawa R, Tang M, Kohno T, Angulo B, Pio R, Montuenga LM, Minna JD, Yokota J, Sanchez-Cespedes M (2009). A Gene-Alteration Profile of Human Lung Cancer Cell Lines. Hum Mutat 30, 1199–1206.

Bourne HR, Sanders DA, McCormick F (1991). The GTPase superfamily: conserved structure and molecular mechanism. Nature 349, 117–127.

Cai H, Das S, Kamimura Y, Long Y, Parent CA, Devreotes PN (2010). Ras-mediated activation of the TORC2-PKB pathway is critical for chemotaxis. J Cell Biol 190, 233–245.

Carmichael J, DeGraff WG, Gazdar AF, Minna JD, Mitchell JB (1987). Evaluation of a tetrazolium-based semiautomated colorimetric assay: assessment of radiosensitivity. Cancer Res 47, 943–946.

Cerami E, Gao J, Dogrusoz U, Gross BE, Sumer SO, Aksoy BA, Jacobsen A, Byrne CJ, Heuer ML, Larsson E, *et al.* (2012). The cBio cancer genomics portal: an open platform for exploring multidimensional cancer genomics data. Cancer Discov 2, 401–404.

Charest PG, Shen Z, Lakoduk A, Sasaki AT, Briggs SP, Firtel RA (2010). A ras signaling complex controls the RasC-TORC2 pathway and directed cell migration. Dev Cell 18, 737–749.

Chen F, Pruett-Miller SM, Huang Y, Gjoka M, Duda K, Taunton J, Collingwood TN, Frodin M, Davis GD (2011). High-frequency genome editing using ssDNA oligonucleotides with zinc-finger nucleases. Nat Methods 8, 753–755.
Collins SE, Wiegand ME, Werner AN, Brown IN, Mundo MI, Swango DJ, Mouneimne G, Charest PG (2023). Ras-mediated activation of mTORC2 promotes breast epithelial cell migration and invasion. Mol Biol Cell 34, ar9.
Fan D, Yu S, Yang Y, Qu S (2021). Low Expression of Rasal2 Promotes Non-small Cell Lung Cancer Metastasis through Ras/ERK Pathway. Biol Pharm Bull 44, 992–998.
Fruman DA, Chiu H, Hopkins BD, Bagrodia S, Cantley LC, Abraham RT (2017). The PI3K Pathway in Human Disease. Cell 605–635.
Fu W, Hall MN (2020). Regulation of mTORC2 Signaling. Genes 11, 1045.
Fujita-Sato S, Galeas J, Truitt M, Pitt C, Urisman A, Bandyopadhyay S, Ruggero D, McCormick F (2015). Enhanced MET Translation and Signaling Sustains K-Ras–Driven Proliferation under Anchorage-Independent Growth Conditions. Cancer Res 75, 2851–2862.
Gan X, Wang J, Su B, Wu D (2011). Evidence for direct activation of mTORC2 kinase activity by phosphatidylinositol 3,4,5-trisphosphate. J Biol Chem 286, 10998–11002.
Gao J, Aksoy BA, Dogrusoz U, Dresdner G, Gross B, Sumer SO, Sun Y, Jacobsen A, Sinha R, Larson E, *et al*. (2013). Integrative analysis of complex cancer genomics and clinical profiles using the cBioPortal. Sci Signal 6, pl1.
Gao Q, Ouyang W, Kang B, Han X, Xiong Y, Ding R, Li Y, Wang F, Huang L,Chen L, *et al*. (2020). Selective targeting of the oncogenic *KRAS* G12S mutant allele by CRISPR/Cas9 induces efficient tumor regression. Theranostics 10, 5137–5153.
Gimple RC, Wang X (2019). RAS: Striking at the Core of the Oncogenic Circuitry. Front Oncol 9, 965.
Giuliano CJ, Lin A, Girish V, Sheltzer JM (2019). Generating Single Cell–Derived Knockout Clones in Mammalian Cells with CRISPR/Cas9. Curr Protoc Mol Biol 128, e100.
Janes MR, Limon JJ, So L, Chen J, Lim RJ, Chavez MA, Vu C, Lilly MB, Mallya S, Ong ST, *et al*. (2010). Effective and selective targeting of leukemia cells using a TORC1/2 kinase inhibitor. Nat Med 16, 205–213.
Kamimura Y, Xiong Y, Iglesias PA, Hoeller O, Bolourani P, Devreotes PN (2008). PIP3-independent activation of TorC2 and PKB at the cell's leading edge mediates chemotaxis. Curr Biol CB 18, 1034–1043.
Khanna A, Lotfi P, Chavan AJ, Montano NM, Bolourani P, Weeks G, Shen X, Briggs SP, Pots H, Van Haastert PJM, *et al*. (2016). The small GTPases Ras and Rap1 bind to and control TORC2 activity. Sci Rep 6, 25823.
Kim LC, Cook RS, Chen J (2017). mTORC1 and mTORC2 in cancer and the tumor microenvironment. Oncogene 36, 2191–2201.
Kim M, Lee E, Kim H, Moon A (2003). p38 kinase is a key signaling molecule for h-Ras-induced cell motility and invasive phenotype in human breast epithelial cells. Cancer Res 63, 5454–5461.
Kovalski JR, Bhaduri A, Zehnder AM, Neela PH, Che Y, Wozniak GG, Khavari PA (2019). The Functional Proximal Proteome of Oncogenic Ras Includes mTORC2. Mol Cell 73, 830–844.e12.
Lauand C, Rezende-Teixeira P, Cortez BA, de Oliveira Niero EL, Machado-Santelli GM (2013). Independent of ErbB1 gene copy number, EGF stimulates migration but is not associated with cell proliferation in non-small cell lung cancer. Cancer Cell Int 13, 38.
Lavoie H, Gagnon J, Therrien M (2020). ERK signalling: a master regulator of cell behaviour, life and fate. Nat Rev Mol Cell Biol 21, 607–632.
Lee KH, Koh M, Moon A (2016). Farnesyl transferase inhibitor FTI-277 inhibits breast cell invasion and migration by blocking H-Ras activation. Oncol Lett 12, 2222–2226.
Liao X-H, Buggey J, Lee YK, Kimmel AR (2013). Chemoattractant stimulation of TORC2 is regulated by receptor/G protein–targeted inhibitory mechanisms that function upstream and independently of an essential GEF/Ras activation pathway in Dictyostelium. Mol Biol Cell 24, 2146–2155.
Lim S, Boyer N, Boo N, Huang C, Venkatachalam G, Juang YCA, Garrigou M, Kaan HYK, Duggal R, Peh KM, *et al*. (2021a). Discovery of cell active macrocyclic peptides with on-target inhibition of KRAS signaling. Chem Sci 12, 15975–15987.
Lim S, Khoo R, Juang YC, Gopal P, Zhang H, Yeo C, Peh KM, Teo J, Ng S, Henry B, *et al*. (2021b). Exquisitely Specific anti-KRAS Biodegraders Inform on the Cellular Prevalence of Nucleotide-Loaded States. ACS Cent Sci 7, 274–291.
Lindsay CR, Jamal-Hanjani M, Forster M, Blackhall F (2018). KRAS: Reasons for optimism in lung cancer. Eur J Cancer 99, 20–27.
Liu GY, Sabatini DM (2020). mTOR at the nexus of nutrition, growth, ageing and disease. Nat Rev Mol Cell Biol 21, 183–203.
Liu P, Gan W, Chin YR, Ogura K, Guo J, Zhang J, Wang B, Blenis J, Cantley LC, Toker A, *et al*. (2015). PtdIns(3,4,5)P3-Dependent Activation of the mTORC2 Kinase Complex. Cancer Discov 5, 1194–1209.
Liu X, Wang P, Zhang C, Ma Z (2017). Epidermal growth factor receptor (EGFR): A rising star in the era of precision medicine of lung cancer. Oncotarget 8, 50209–50220.
Liu Z, Zhao M, Jiang X, Zhang Y, Zhang S, Xu Y, Ren H, Su H, Wang H, Qiu X (2022). Upregulation of KLHL17 promotes the proliferation and migration of non-small cell lung cancer by activating the Ras/MAPK signaling pathway. Lab Invest 102, 1389–1399.
Lone M-U-D, Miyan J, Asif M, Malik SA, Dubey P, Singh V, Singh K, Mitra K, Pandey D, Haq W, *et al*. (2019). Direct physical interaction of active Ras with mSIN1 regulates mTORC2 signaling. BMC Cancer 19, 1236.
Mitsudomi T, Yatabe Y (2010). Epidermal growth factor receptor in relation to tumor development: EGFR gene and cancer. FEBS J 277, 301–308.
Moon A, Kim M-S, Kim T-G, Kim S-H, Kim HE, Chen YQ, Choi KIM H-R (2000). H-RAS, but not N-RAS, induces an invasive phenotype in human breast epithelial cells: a role for MMP-2 in the H-RAS-induced invasive phenotype. J Cancer 85, 176–181.
Muñoz-Maldonado C, Zimmer Y, Medová M (2019). A Comparative Analysis of Individual RAS Mutations in Cancer Biology. Front Oncol 9, 1088.
Omerovic J, Hammond DE, Clague MJ, Prior IA (2008). Ras isoform abundance and signalling in human cancer cell lines. Oncogene 27, 2754–2762.
Pal DS, Banerjee T, Lin Y, de Trogoff F, Borleis J, Iglesias PA, Devreotes PN (2023). Actuation of single downstream nodes in growth factor network steers immune cell migration. Dev Cell 58, 1170–1188.e7.
Pawig L, Klasen C, Weber C, Bernhagen J, Noels H (2015). Diversity and Inter-Connections in the CXCR4 Chemokine Receptor/Ligand Family: Molecular Perspectives. Front Immunol 6, 429.
Phillips RJ, Burdick MD, Lutz M, Belperio JA, Keane MP, Strieter RM (2003). The stromal derived factor-1/CXCL12-CXC chemokine receptor 4 biological axis in non-small cell lung cancer metastases. Am J Respir Crit Care Med 167, 1676–1686.
Prior IA, Hood FE, Hartley JL (2020). The Frequency of Ras Mutations in Cancer. Cancer Res 80, 2969–2974.
Pylayeva-Gupta Y, Grabocka E, Bar-Sagi D (2011). RAS oncogenes: weaving a tumorigenic web. Nat Rev Cancer 11, 761–774.
Rathinaswamy MK, Burke JE (2020). Class I phosphoinositide 3-kinase (PI3K) regulatory subunits and their roles in signaling and disease. Adv Biol Regul 75, 100657.
Rhett JM, Khan I, O'Bryan JP (2020). Chapter Three - Biology, pathology, and therapeutic targeting of RAS. In: Advances in Cancer Research, ed. Tew KD, Fisher PB, Cambridge, CA: Academic Press, 69–146.
Saha S, Town JP, Weiner OD (2023). Mechanosensitive mTORC2 independently coordinates leading and trailing edge polarity programs during neutrophil migration. Mol Biol Cell 34, ar35.
Sasaki AT, Firtel RA (2006). Regulation of chemotaxis by the orchestrated activation of Ras, PI3K, and TOR. Eur J Cell Biol 85, 873–895.
Sayed S, Sidorova OA, Henning A, Augsburg M, Cortés Vesga CP, Abohawya M, Schmitt LT, Sürün D, Stange DE, Mircetic J, *et al*. (2022). Efficient Correction of Oncogenic KRAS and TP53 Mutations through CRISPR Base Editing. Cancer Res 82, 3002–3015.
Senoo H, Kamimura Y, Kimura R, Nakajima A, Sawai S, Sesaki H, Iijima M (2019). Phosphorylated Rho–GDP directly activates mTORC2 kinase towards AKT through dimerization with Ras–GTP to regulate cell migration. Nat Cell Biol 21, 867–878.
Sheffels E, Kortum RL (2021). The Role of Wild-Type RAS in Oncogenic RAS Transformation. Genes 12, 662.
Simanshu DK, Nissley DV, McCormick F (2017). RAS Proteins and Their Regulators in Human Disease. Cell 170, 17–33.
Singh A, Greninger P, Rhodes D, Koopman L, Violette S, Bardeesy N, Settleman J (2009). A Gene Expression Signature Associated with "K-Ras Addiction" Reveals Regulators of EMT and Tumor Cell Survival. Cancer Cell 15, 489—500.
Smith SF, Collins SE, Charest PG (2020). Ras, PI3K and mTORC2 – three's a crowd? J Cell Sci 133, jcs234930.
Soriano O, Alcón-Pérez M, Vicente-Manzanares M, Castellano E (2021). The Crossroads between RAS and RHO Signaling Pathways in Cellular Transformation, Motility and Contraction. Genes 12, 819.
Tate JG, Bamford S, Jubb HC, Sondka Z, Beare DM, Bindal N, Boutselakis H, Cole CG, Creatore C, Dawson E, *et al*. (2019). COSMIC: the Catalogue Of Somatic Mutations In Cancer. Nucleic Acids Res 47, D941–D947.
Tee AR (2018). The Target of Rapamycin and Mechanisms of Cell Growth. Int J Mol Sci 19, 880.

Uekita T, Fuji S, Miyazawa Y, Iwakawa R, Narisawa-Saito M, Nakashima K, Tsuta K, Tsuda H, Kiyono T, Yokota J, *et al*. (2014). Oncogenic Ras/ERK Signaling Activates CDCP1 to Promote Tumor Invasion and Metastasis. Mol Cancer Res 12, 1449–1459.
Wang Z, Sun J, Feng Y, Tian X, Wang B, Zhou Y (2016). Oncogenic roles and drug target of CXCR4/CXCL12 axis in lung cancer and cancer stem cell. Tumour Biol J Int Soc Oncodevelopmental Biol Med 37, 8515–8528.
Weng M-T, Lee J-H, Wei S-C, Li Q, Shahamatdar S, Hsu D, Schetter AJ, Swatkoski S, Mannan P, Garfield S, *et al*. (2012). Evolutionarily conserved protein ERH controls CENP-E mRNA splicing and is required for the survival of KRAS mutant cancer cells. Proc Natl Acad Sci 109, E3659–E3667.
Westcott PMK, Halliwill KD, To MD, Rashid M, Rust AG, Keane TM, Delrosario R, Jen KY, Gurley KE, Kemp CJ, *et al*. (2015). The mutational landscapes of genetic and chemical models of Kras-driven lung cancer. Nature 517, 489–492.
Westcott PMK, To MD (2013). The genetics and biology of KRAS in lung cancer. Chin J Cancer 32, 63–70.
Xie J, Wang X, Proud CG (2018). Who does TORC2 talk to? Biochem J 475, 1721–1738.
Xie S, Zeng W, Fan G, Huang J, Kang G, Geng Q, Cheng B, Wang W, Dong P (2014). Effect of CXCL12/CXCR4 on increasing the metastatic potential of non-small cell lung cancer in vitro is inhibited through the downregulation of CXCR4 chemokine receptor expression. Oncol Lett 7, 941–947.
Yoh KE, Regunath K, Guzman A, Lee S-M, Pfister NT, Akanni O, Kaufman LJ, Prives C, Prywes R (2016). Repression of p63 and induction of EMT by mutant Ras in mammary epithelial cells. Proc Natl Acad Sci 113, E6107–E6116.
Young A, Lou D, McCormick F (2013). Oncogenic and wild-type ras play divergent roles in the regulation of mitogen-activated protein kinase signaling. Cancer Discov 3, 113–123.
Zhang Z, Guiley KZ, Shokat KM (2022). Chemical acylation of an acquired serine suppresses oncogenic signaling of K-Ras(G12S). Nat Chem Biol 18, 1177–1183.
Zhou B, Der CJ, Cox AD (2016). The role of wild type RAS isoforms in cancer. Semin Cell Dev Biol 58, 60–69.
Zhou H, Huang S (2010). The Complexes of Mammalian Target of Rapamycin. Curr Protein Pept Sci 11, 409–424.
Zhu Q-G, Zhang S-M, Ding X-X, He B, Zhang H-Q (2017). Driver genes in non-small cell lung cancer: Characteristics, detection methods, and targeted therapies. Oncotarget 8, 57680–57692.
Zuo J, Wen M, Li S, Lv X, Wang L, Ai X, Lei M (2017). Overexpression of CXCR4 promotes invasion and migration of non-small cell lung cancer via EGFR and MMP-9. Oncol Lett 14, 7513–7521.